COLOUR HELIUM BUBBLE FLOW VISUALIZATION TECHNIQUE

ICAS-86-1.7.1

Zhao Dong, Wang Zhongqi, Zhang Xiaodi,
Qin Jialin and Lang Xianzhong
Harbin Aerodynamic Research Institute (China)

Abstract

Colour helium bubble flow visualization is a new and unique technique. Flow visualization in the wind tunnel using colour helium bubble has recently been achieved at Harbin Aerodynamic Research Institute. The colour bubble film solution developed by us and used colour light source and method of colour visualization have success. Rich and varied colour paths are obtained. The clear and gay colour video tape recording and colour photographs are taken.

This paper describes unique principle of light interference for flow visualization with colour helium bubble. The different colours of colour helium bubble depend opon wevelenghth of light, refractive index and thickness of bubble film and angle of reflection in the bubble film. Controlled methods of this four paramaters are indicated. A formula of the bubble film thickness calculation is derived. The corresponding relation between the bubble film thickness and other paramater is calculated by us using numerical calculation. The calculated result is described. The typical flow visualization photographs are presented. Objective appraisal of significance with colour helium bubble flow visualization is given.

Introduction

Helium bubble flow visualization is one of the important visualization techniques of flow patterns on wind tunnel models. It is well-known that a helium-filled bubble generator is used to produce neutrally-buoyant bubbles which, when emitted into the freestream forward of the model, would reveal the general flow about the model. A high-intensity light source is placed behind the model and directed upstream such that the bubbles would appear white in contrast to the black surfaces of the model and background (wind tunnel wall). With the result that the stereoscopic flow pattern on wind tunnel models is clear at a glance[1]. At present monochromatic helium bubble flow visualization technique has been extensivily applied to the physical study of flow on wind tunnel models in many countries.

The monochromatic helium bubble flow visualization was realized in July 1982 at Harbin Aerodynamic Research Institute. After that the colour helium bubble flow visualization was successfully realized in March 1984. The colour bubble film solution developed by us and used colour light source and method of colour visualization have success. Rich and varied colour paths are obtained. The clear and gay colour video tape recording and colour photographs are taken.

Just as dye lines of different colours have an advantage over the monochromatic ones in water tunnel, so the colour helium bubble have precedence over monochromatic one for flow visualization in wind tunnel; because the resolving power of people and apparatus on colour has precedence over that on grey level. In comparison with colour dye lines in water tunnel, the colour helium bubble flow visualization technique in wind tunnel can be realized at higher Reynolds numbers; moreover, for unsteady flowfield qualitative visualization can be realized and quantitative information can be obtained[2]. As concerns the resolving power, the colour helium bubble is higher than the monochromatic one. So the use of the colour helium bubble can raise efficiency and benefit greatly for flow visualization test in wind tunnel. As above, the colour helium bubble flow visualization technique will has a bright future for wide use.

Principle of Colour Visualization

Appearances of different colours of helium bubbles are arised from interference of light. Helium bubble film thickness are as thin as wafer, which are about 0.5 μ to 1 μ within the reach of the flow visualization. Surface of film is a curved one. Thicknesses are not equal in different position. Thus, study of light interference phenomenon for helium bubble is complicated.

Suppose a transparant film with plane reflecting surfaces. not necessarily parallel, is illuminated by a point source S of quasi-monochromatic light. Two rays* from S namely SAP and SBCDP (Fig 1), reach

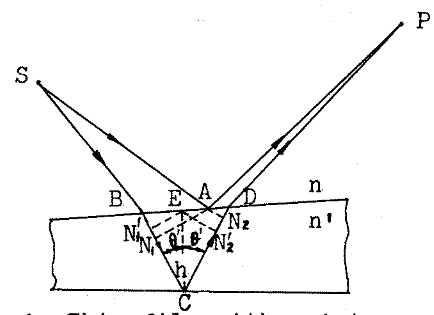

Figure 1. Thin film with point source

*We neglect multiple reflections.

any point P on the same side of the film as S, so that there is a non-localized interference pattern in this region. The difference between these two optical paths from S to P is

$$\Delta\phi = n(SB+DP-SA-AP)+n'(BC+CD), \qquad (1)$$

where n', n are respectively the refractive indices of the film and of the surrounding medium(3). The exact value of may be difficult to calculate, but if the film is sufficiently thin, B, A and D are close together on the upper surface, so that

$$nSA \doteq nSB + n'BN_1, \qquad (2)$$

and

$$nAP \doteq nDP + n'N_2D, \qquad (3)$$

where AN_1, AN_2, are respectively perpendicular to BC, CD. From (1), (2) and (3)

$$\Delta\phi \doteq n'(N_1C + CN_2). \qquad (4)$$

Further, if the angle between the surfaces of the film is sufficiently small,

$$N_1C + CN_2 \doteq N_1'C + CN_2', \qquad (5)$$

where N_1', N_2' are respectively the feet of perpendiculars from E to BC, CD; and E is the intersection with upper surface at C. Now

$$N_1'C = CN_2' = \cos\theta', \qquad (6)$$

where h=CE is the thickness of the film at C, measured normal to the lower surface, and θ' is the angle of reflection in the film. Hence for a thin film of small angle we may write, from (4), (5) and (6)

$$\Delta\phi = 2n'h\cos\theta', \qquad (7)$$

and the corresponding phase difference at P is

$$\delta = \frac{4\pi}{\lambda_0} n'h\cos\theta', \qquad (8)$$

where λ_0 is the wavelength of light.

In general, for a given P, both h and θ' vary with the position of S, and a small extension of the source makes the range of δ at P so large that the fringes disappear. There is, however, a special case when P is in the film, as when observations are made with a microscope focused on the film, or with the eye accommodated for it. Under these circumstances h is practically the same for all pairs of rays from an extended source reaching P', conjugate to P (Fig 2), and difference of at P' are due mainly to differences of $\cos\theta'$. If the range of value of $\cos\theta'$ is sufficiently small, the range of δ at P' may be much less than 2π even with a source of appreciable extension, and distinct fringes are then visible, apparently localized in the film. In practice, the condition of a small range of $\cos\theta'$ can be

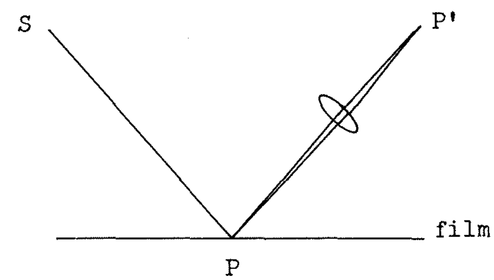

Figure 2. Thin film: illustrating formation of fringe localized in the film

satisfied by observing near normal incidence, and also by pupil of the unaided eye may itself be sufficiently small. Taking into account the phase change of π on reflection at one of the surfaces of the film, there are maxima of intensity at P' (and so apparantly at P) when

$$2n'h\,\overline{\cos\theta'} \pm \frac{\lambda_0}{2} = m\lambda, \quad m = 0,1,2, \ldots, \qquad (9)$$

and minima of intensity when

$$2n'h\,\overline{\cos\theta'} \pm \frac{\lambda_0}{2} = m\lambda, \quad m = \frac{1}{2},\frac{3}{2},\frac{5}{2}, \ldots, \qquad (10)$$

where $\overline{\cos\theta'}$ is a mean value of $\cos\theta'$ for the points of the source which contribute light to P'. The quantity n'h which appears in these relations is the optical thickness of the film at P; as far as our aprroximations are instified the state of interference at P is unaffected by the film thickness elsewhere. It follows that (9), (10) holds even if the bounding surfaces of the thin film are not plane, so long as the angle between them remains small. If a source of white light is used, the interference fringes of surface for helium bubble are coloured ones.

Method of Colour Visualization

From (7) and (8), the different colours of colour helium bubble are dependent upon n', h, θ', and λ_0. In reality, the key to the settlement of the colour helium bubble flow visualization technique lies in control of this four paramaters.

As concerns the light source, firstly, the intensity of light must be high enough; secondly, this technique requeres as wide wavelength region as possible, to achieve rich and varied colours. Our colour light source can satisfy satisfactorily the need of the colour helium bubble flow visualization.

Only for some spesific refractive indices of film can obtain the different colours and so only a part of the various bubble film solution is valid for appearance of colour. In fact, our bubble film solution (such as BFS 1110, BFS 1120, BFS 2115 and BFS 4120) used with the monochromatic helium bubble flow visualization did not obtain the colours. By use of colour bubble film solution CPY 240-3 developed by us the rich and varied colours are obtained. The bubble generation rate was increased substantially over what we had obtained previously. Furthermore, it is not toxic, corrosive or likely to stain anything.

The angle of reflection in the film must be confined within necessary limits. If the varying range of θ' is too large, various colours will appear for identical bubble in different positions. If so, the different bubble's paths can not be distinguished by their own colours. Thus, the position and mutual distances of the colour light source. model and head must be arranged reasonably.

The colour helium bubble flow visualization technique requires the range of film thickness distribution wide enough to obtain the rich and varied colours at an instantaneousness. For this reason the control of the film thickness h is important, which is to be discussed later in detail.

Calculation and Control of the Bubble Film Thickness

Since the bubbles are filled with helium and thus neutrally buoyant, they would follow flow faithfully. As a consequence, the weight of the helium bubble should equal to that of air with the same volume; i.e.,

$$\gamma_B v_B + \gamma_H v_H = \gamma_K v_K , \qquad (11)$$

where γ is specific gravity and v is volume. The foodhotes $_B$, $_H$ and $_K$ indicate the bubble film solution, helium and air respectively. Assume that helium bubble is a globular shape, then equation (11) can be written in the form

$$\frac{4\pi}{3}\left[r^3-(r-h)^3\right] \gamma_B + \frac{4\pi}{3}(r-h)^3 \gamma_H = \frac{4\pi}{3} r^3 \gamma_K , \qquad (12)$$

where r is the radius of the helium bubble and h is the thickness of the film. After the substitution of γ_B, γ_H and γ_K in equation (12) and making the equation simplify, we have

$$Ah^3 - Brh^2 + Cr^2 h - Dr^3 = o, \qquad (13)$$

where A, B, C and D are constants. From equation (13) we can find that the relation between h and r. Make r an independent variable, then equation (13) is a monadical cubic equation. First of all, in the numerical calculation the approximate solution h_o is extracted by us using numerical-graphic method to approximate the exact solution h quickly. Assume that the exact solution of the film thickness is $h_o+\Delta h$, i.e., $h=h_o+\Delta h$, then equation (13) can be written in the form

$$f(h_o+\Delta h) = 0. \qquad (14)$$

In order to be able to determine the equation (14) by the use of the Taylor formula, we expand the left side of equation (14) in the power series

$$f(h_o+\Delta h)=f(h_o)+f'(h_o)\Delta h+\frac{f''(h_o)}{2!}\Delta h^2 + \ldots$$

$$\frac{f^{(n-1)}(h_o)}{(n-1)!}\Delta h^{n-1} + \frac{f^{(n)}(c)}{n!}\Delta h^n , \qquad (15)$$

where $h_o \lessgtr c \gtrless h_o+\Delta h$. Since Δh is very small and thus second degree term and higher of Δh can be omitted from equation (15). we now have

$$f(h_o+\Delta h)=f(h_o)+f'(h_o)\Delta h= 0, \qquad (16)$$

and hence

$$\Delta h=-\frac{f(h_o)}{f'(h_o)}, \qquad (17)$$

where

$$f(h_o)=Ah_o^3-Brh_o^2+Cr^2 h_o-Dr^3 , \qquad (18)$$

and

$$f'(h_o)=3Ah_o^2-2Brh_o+Cr^2 . \qquad (19)$$

After the calculation of Δh, the film thickness $h_1=h_o+\Delta h$ of first approximate calculation can be extracted. After this, substitate h_o by h_1 that we conduct approximate calculation for the second time. In general, $\Delta h<10^{-7}$ mm can be achieved by double approximation. When calculating h corresponding to other r, it is not needed again to apply numerical-graphic method. The approximate solution h_o corresponding to some r can be fetched from known h near to this r. Thus, calculating work load and time can be saved greatly.

The calculated result for relation between the film thickness and the diameter of bubble is shown in Fig 3. From which we

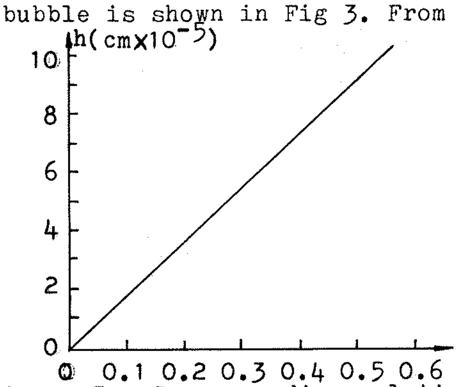

Figure 3. Corresponding relation between the film thickness and the diameter of bubble

can see that the relation between h and d is linear. In practice, we can control the film thickness by controlling the diameter of bubble. Hence we can obtain the requisite film thickness by controlling the parametric distributions of compressed air, helium and bubble film solution.

At some instant the bubble diameter distribution is not unitary. In our routine condition the date of generated bubbles per second are shown in table 1. From

Diameter (cm)	Quantity	Percentage
0.5	46	11.5 %
0.4	44	11 %
0.2, 0.3	256	65 %
0.1	50	12.5 %

TABLE 1 PARAMETERS OF GENERATED BUBBLES

which we can see that the diameters are different. When keep constancy of the parameter distributions of compressed air, helium and bubble film solution, there are various sized bubbles simultaneously. Of cource, film thickness of bubble are different too (see table 2). With the result that the different colours are ensured.

Typical Flow Visualization Photographs

Figure 4 to 7 present photographs of the colour helium bubble flow visualization of the 1/21-scale YF-16 model. The wind tunnel is a low speed open return tunnel. The test section has diameter of 1500 milimetres, length of 1950 milimetres. The wind tunnel is operated at a

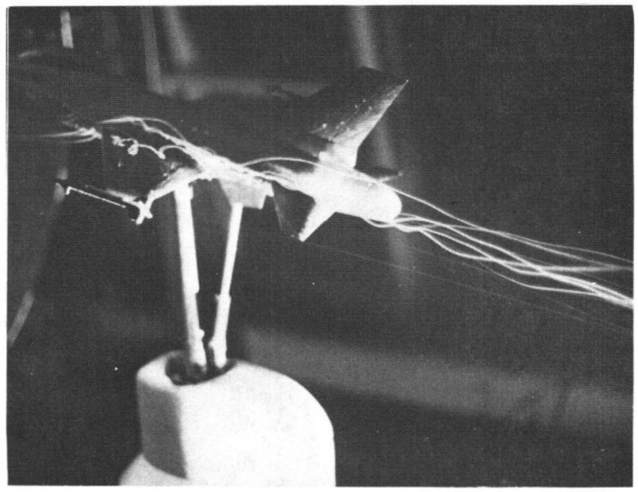

Figure 5. Colour Helium Bubble Visualization Photograph for $\alpha=14°$

test section velocity of 10 meter per second. Fegures 4 to 6 and 7 present resuits obtained for $\alpha=14°$, and $\alpha=8°$, respectively, where α is angle of attack. Figures 5 and 6 present patterns of the strake vortex and of the wing leading edge vortex. Figures 4 and 7 show that patterns of latter half of the strake vortex and of the outside vortex.

From these photographs we can see that

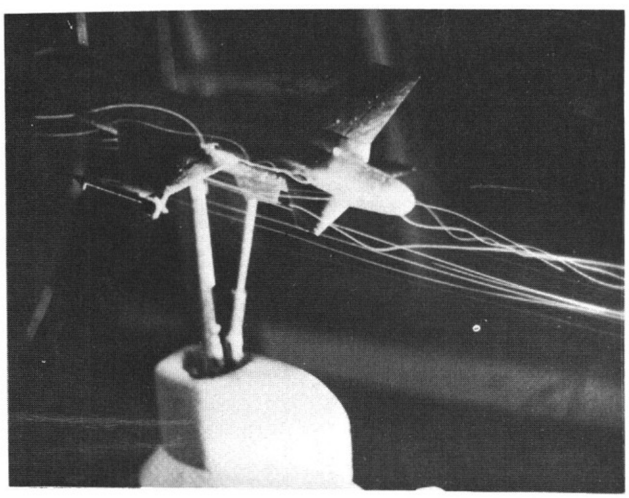

Figure 4. Colour Helium Bubble Visualization Photograph for $\alpha=14°$

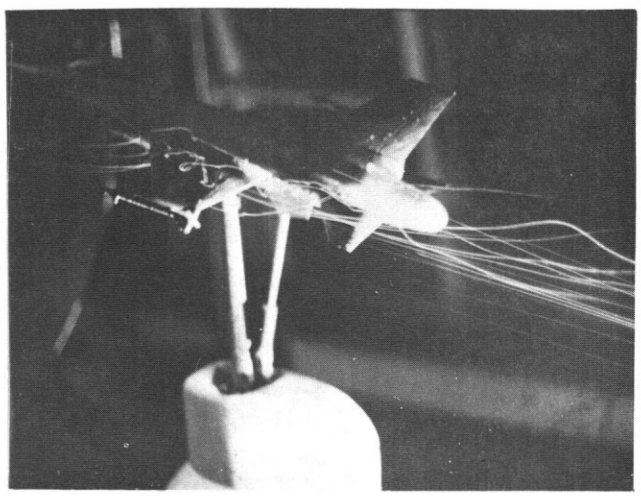

Figure 6. Colour Helium Bubble Visualization Photograph for $\alpha=14°$

Diameter (cm)	0.1	0.2	0.3	0.4	0.5
Film Thickness (cm)	$1.847\ 10^{-5}$	$3.679\ 10^{-5}$	$5.547\ 10^{-5}$	$7.395\ 10^{-5}$	$9.245\ 10^{-5}$

TABLE 2 FILM THICKNESS OF GENERATED BUBBLES

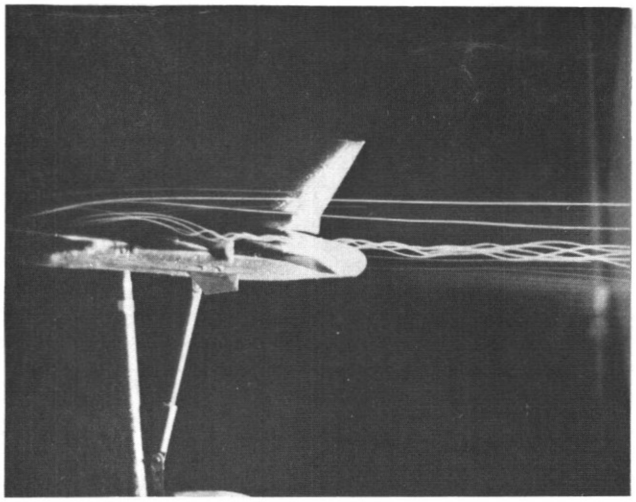

Figure 7. Colour Helium Bubble Visualization Photograph for $\alpha=8^\circ$

colour helium bubble has precedence over the monochromatic one for flow visualization. The stream lines of the different colour can be resolved easily, espesially for the condition of a lot of stream lines mingle each other. Thus, for complex three dimensional flow fields the colour helium bubble flow visualization technique is completely qualified, whether for qualitative visualization or for quantitative measurement.

Conclusions

Flow visualization using colour helium bubble in wind tunnel is a new and unique technique. Emergence of this technique makes stereoscopic and colour flow visualization achieve in air, moreover, in comparison with the colour dye lines in water tunnel, which can be realized at higher Reynolds numbers. Furthermore, for unsteady flofield the qualitative visualization can be realized and the quantitative information can be obtained.

The colour bubble film solution developed by us and used colour light source and method of colour visualization ensure the reasonable values of $\lambda_\circ$, n', h and θ'. Rich and varied colour helium bubble paths are obtained. The resolving powers of people and apparatus on varied paths are increased greatly. The clear and gay colour video tape recording and colour photographs are taken. Thus, colour helium bubble flow visualization technique is important, whether for qualitative visualization or for quantitative measurement.

References

(1) R. W. Hale, P. Tan, P. C. Stowell and D. E. Ordway: "Development of an Integrated System for Flow Visualization in Air Using Neutrally-Buoyant Bubbles," AD 756691 December 1971.

(2) David F. Rogers: "Quantitative Information from Helium Bubble Flow Visualization Using Computer Graphics Techniques," AIAA Paper No 76-93. January 1976.

(3) Max Born and Emal Wolf: "Principles of Obtics," (5th ed) Pergaman Press, 1975.